

Comprehensive routing strategy on multilayer networks

Lei Gao,^{1,2} Panpan Shu,³ Ming Tang*,^{1,2,4} Wei Wang^{†,1,2} and Hui Gao^{1,2}

¹Web Sciences Center, University of Electronic Science and Technology of China, Chengdu 610054, China

²Big data research center, University of Electronic Science and Technology of China, Chengdu 610054, China

³School of Sciences, Xi'an University of Technology, Xi'an 710054, China

⁴School of Information Science Technology, East China Normal University, Shanghai 200241, China

(Dated: September 1, 2018)

Designing an efficient routing strategy is of great importance to alleviate traffic congestion in multilayer networks. In this work, we design an effective routing strategy for multilayer networks by comprehensively considering the roles of nodes' local structures in micro-level, as well as the macro-level differences in transmission speeds between different layers. Both numerical and analytical results indicate that our proposed routing strategy can reasonably redistribute the traffic load of the low speed layer to the high speed layer, and thus the traffic capacity of multilayer networks are significantly enhanced compared with the monolayer low speed networks. There is an optimal combination of macro- and micro-level control parameters at which can remarkably alleviate the congestion and thus maximize the traffic capacity for a given multilayer network. Moreover, we find that increasing the size and the average degree of the high speed layer can enhance the traffic capacity of multilayer networks more effectively. We finally verify that real-world network topology does not invalidate the results. The theoretical predictions agree well with the numerical simulations.

PACS numbers: 89.75.Hc, 89.75.Fb, 89.40.-a

Alleviating the congestion in transportation and communication systems is vital to modern society. For the purpose of redistributing the traffic load in a low speed transportation system such as bus net, we can establish a high speed system (e.g., subway network) in the busy regions or between the stations with high traffic flow, and the two systems make up a new multilayer system (i.e., multilayer network). Recent years, some investigations about traffic congestion on multilayer networks were performed, which mainly focused on the different roles of layers in a macroscopic level (e.g., different transmission speeds), or the local structures of nodes within the same layer in a microscopic level, without taking them into consideration comprehensively. To this end, we propose a comprehensive routing strategy on multilayer networks composed of a low and a high speed network. We introduce a macro- and a micro-level parameter to adjust the roles of network structures played in the routing strategy. Our strategy redistributes the traffic load in low speed layer to the high speed layer reasonably, and the traffic capacity of multilayer networks are thus remarkably enhanced compared with the monolayer low speed networks. For a given multilayer network, an optimal combination of macro- and micro-level parameters is found. Under these parameters, the traffic capacity of the system reaches its maximum value. Moreover, increasing the networks size and the average degree of the high speed layer can enhance the traffic capacity of multilayer networks more effectively. To quantificationally understand the proposed routing strategy, we developed a theoretical approach and a remarkable agreement with numerics is observed in both artificial

and real-world networks. Our research may stimulate future studies on designing realistic transportation and communication multilayer networks.

I. INTRODUCTION

Many systems in modern society can be described by complex networks, such as power grids, transportation networks and social networks [1–5]. Routing on such networked systems to enhance traffic capacity is a significant issue, and has been widely studied from the perspective of complex network framework over the past decades [6–11]. Most studies about routing are focused on monolayer networks. The studies have revealed that traffic congestion is highly related to the structures of networks [3, 12, 13]. Generally, there are three widely used techniques to enhance the throughput of the whole network: (1) modification of network structures [14–17], (2) optimization of traffic resources allocations [18–20], and (3) designing better routing strategies [9, 21–27]. Compare with the first two methods, proposing effective routing strategies seems to be more practical and thus has attracted much interest. Among numerous different kinds of proposed routing strategies, an efficient routing strategy proposed by Yan and his colleagues is widely acknowledged for its simplicity and efficiency [21]. The strategy redistributes traffic load in central nodes to other noncentral nodes and improves the network throughput significantly. Echenique *et al.* proposed a novel traffic awareness protocol (TAP) by considering the waiting time of packets, in which a node forwards a packet to its neighboring node according to the shortest effective distance [28, 29]. Some scholars also proposed strategies for systems with limited band width [30, 31].

With the availability of big data, scholars found that modern infrastructures are actually significantly interact with and/or depend on each other, which can be described as multilayer

*Correspondence to: tangminghan007@gmail.com

†Correspondence to: wwzqbx@hotmail.com

(multiplex) networks [32–35]. For example, to redistribute the traffic load in a low speed transportation network, we can build a new high speed network in the busy regions or between the high flow stations, and the two monolayer networks constitute a multilayer network. Researchers have demonstrated that the dynamics of [35] and on [36–39] multilayer networks are markedly different from monolayer networks. Until very recently, some researchers studied the traffic dynamics on multilayer complex networks, i.e., how to alleviate the traffic congestion in order to enhance the multilayer network capacity [40–45]. Interestingly, Solé-Ribalta *et al.* [44] developed a standardized model of transportation in multilayer networks, and showed that the structure of multiplex networks can induce congestion on account of the unbalance of shortest paths between layers. Morris and Barthélemy [40] analyzed a multilayer network consists of two layers, and showed that it is possible to obtain an optimal communication multiplex by balancing the effects between decreasing the average distance and congestion on a very small subset of edges.

The structures of multilayer networks bring new challenges when we propose effective routing strategies, and the task is markedly different from monolayer networks. On one hand, multilayer networks can relieve the traffic congestion of the low speed layer by using the high speed layer, however congestion may be induced in the high speed layer [46]. Although establishing high speed transportation networks can improve the traffic capacity of low speed network, how to reasonably redistribute traffic loads is an essential issue. On the other hand, when designing effective routing strategies we should (1) take the intra-layer structures into considerations from microscopic perspective, and (2) consider the efficiencies of different layers from a macroscopic view. Previous investigations about traffic congestion on multilayer networks mainly focused on the macroscopic differences between layers [40], or the local structure of nodes within the same layer in a microscopic level [43], without taking both of them into consideration comprehensively. In this work, we propose an comprehensive routing strategy on multilayer networks by incorporating the macroscopic difference of speed between layers and microscopic distinctions among different nodes in the same layer. We find that our routing strategy can redistribute the traffic load in low speed layer to high speed layer reasonably, and the traffic capacity of multilayer networks are remarkably enhanced compared with the monolayer low speed networks. For a given multilayer network, there is an optimal combination of macro-level parameter and micro-level parameter that maximize the traffic capacity. Increasing the size and average degree of the high speed layer can enhance the traffic capacity of multilayer networks more effectively. Numerical results on artificial multilayer networks as well as the real Work-Facebook multilayer network agree well with our analysis.

The outline of the paper is as follows. In Sec. II, we give a detailed description of our routing strategy on multilayer networks. In Sec. III, we suggest theoretical analysis. In Sec. IV, we present our simulation results. Section V summarizes our results and conclusions.

II. MODEL

A. Network model

The multilayer network considered is composed by two layers with N_A and N_B nodes respectively. Layer A represent the low speed network, and layer B is the high speed network. In general condition, the expense of building a high speed network is far more than that of low speed network, thus the size of high speed network is smaller. For example, in the railway-airline multilayer network, where the speed (cost) of the airline network is faster (more) than that of the railway network. Thus, the size of the airline network is smaller than the railway network, and all airline stations are located at points which can be considered as nodes in the railway network, but no vice versa [47]. For simplicity, we assume that the nodes in the high speed layer B are a random subset of the low speed layer A [40]. We use the uncorrelated configuration model (UCM) [48] to generate the low speed layer A , and use the Erdős-Rényi (ER) networks [49] to represent the high speed layer B . The multilayer network is generated as follows: (1) Build layer A using the UCM method with power-law degree distributions $P(k) \sim k^{-\gamma}$, where γ is the degree exponent. We set the size of layer A as N_A , the minimum degree is $k_{\min} = 2$, and the maximum degree is $k_{\max} \sim \sqrt{N_A}$. (2) Randomly select N_B ($N_B \leq N_A$) nodes in layer A , and match these nodes one-to-one. This means that each pair of the two matched nodes v_A^o and v_B^o are actually the same node but in two different transport manners. Both of them can be denoted as a coupled node v^o . Or say, a coupled node v^o has two replica nodes in layers A and B , which are denoted by v_A^o and v_B^o respectively. (3) Construct a ER network as the second layer B by using the selected N_B nodes in step (2), i.e., each pair of these randomly selected nodes are connected with a probability p . According to the above three steps, a multilayer network can be built. Note that every node in layer B has its counterpart node in layer A , but the inverse is not true. We denote the degree distribution of the multilayer network as $P(\vec{K}) = P(k_A, k_B)$, where k_A and k_B denote the degrees in layer A and B respectively. For a node v_A in layer A without counterpart in layer B , we have $k_B = 0$. An illustration of the multilayer network is shown in Fig. 1(a).

B. Routing model

In our model, we assume all nodes in layer A are treated as both hosts and routers for generating and delivering packets, while the nodes in layer B can only deliver packets. We assume that a coupled node v^o can deliver packets between layers with infinity bandwidth and no time consumption through two replica nodes v_A^o and v_B^o . For simplicity, each node in the layer A (B) has the same maximum packet delivery ability C_A (C_B). That's to say, at each time step each node v_A can delivery C_A packets to its neighbors in layer A if it has no counterpart in layer B . Otherwise, its counterpart node v_B can also transmit C_B packets in layer B . We set $C_A = C_B = C = 1$

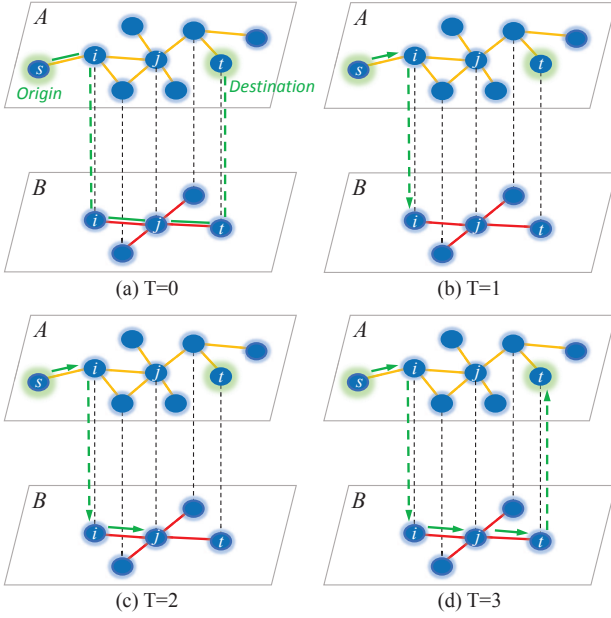


FIG. 1: An illustration of multilayer network where the nodes of layer B form a subset of the nodes of network A . Edges of layer A are shown in orange, edges of network B are shown in red, and nodes in common to both layers are considered to be coupled nodes (shown by dashed lines). Highlighted in green, a path between the ‘origin’ s and the ‘destination’ t is represented, and the arrows show a packet delivery process on the path without congestion. Coupled nodes can deliver packets between layers with no time consumption. (a) At $T = 0$, a packet is generated with the randomly chosen ‘origin’ s and ‘destination’ t in layer A , and a path (highlighted in green) from node s to t is chosen according to the pre-given routing strategy. (b) $T = 1$, ‘origin’ s delivers the packet to the next stop i through the edge (s, i) in layer A . (c) $T = 2$, node i delivers the packet to the next stop j through the edge (i, j) in layer B . (d) $T = 3$, node j delivers the packet to its ‘destination’ t through the edge (j, t) in layer B , and the packet is removed from the system.

in this paper for simplicity.

Due to the finite delivery ability of nodes, a queue of buffers is needed for each node to accommodate packets waiting for being delivered. The transport processes is as follows:

1. Packet generation. At each time step, R number of packets are generated with randomly chosen origins and destinations in layer A . For each packet, a path from the source to the destination is chosen according to the comprehensive multilayer routing strategy (to be introduced in the next subsection). If there are several paths between these two nodes, we choose one randomly. Each newly created packet is placed at the end of the queue of its source node v_A if the next stop is in layer A , or queued at the counterpart node v_B if the next stop is in layer B .
2. Packet processing. The first-in-first-out (FIFO) rule is adopted to hand each queue. At each time step, node v_A (v_B) can process $C_A = 1$ ($C_B = 1$) packet from the

head of its queue and deliver the packet to the next stop in layer A (B). So a coupled node v^o at most process 2 packets per time step through two replica nodes v_A^o and v_B^o in layers A and B . For a non-coupled node v_A (i.e., node v_A has no counterpart in layer B), it can process only $C_A = 1$ packet. When a packet arrives at its destination, it is removed from the system; otherwise it is queued.

C. Comprehensive multilayer routing strategy

By integrating different roles of nodes in micro-level, as well as different transmission speed of layers in macro-level, we propose a comprehensive multilayer routing (CMR) strategy, which can remarkably enhance the traffic capacity of multilayer networks. We denote that a path between nodes s and t as

$$p(s \rightarrow t) := s \equiv v_F^0, v_F^1, \dots, v_F^l, \dots, v_F^{d-1}, v_F^d \equiv t, \quad (1)$$

where v_F^l is the l -st stop and node v_F^l belongs to layer $F \in \{A, B\}$, and d is the number of stops in this path. Similar to Ref. [21], we denote an ‘efficient path’ for any path between nodes s and t as

$$L(p(s \rightarrow t), \alpha_F, \beta_F) = \sum_{l=0}^{d-1} \alpha_F [k(v_F^l)]^{\beta_F}. \quad (2)$$

where $k(v_F^l)$ is the degree of node v_F^l in layer F . The efficient path between s and t is corresponding to the route that makes the sum $L(p(s \rightarrow t), \alpha_F, \beta_F)$ minimum. If there are several efficient paths between two nodes, we choose one randomly. The efficient path is related to the macro-parameter α_F and micro-parameter β_F . The macro-parameter $\alpha_F \geq 0$ controls packet transmission speed in layer F , and reflects the macro-level transmission speed difference between layers. The smaller value of α_F , the faster transmission in layer F . The parameter α_A (α_B) corresponds to the slower (faster) network and the ratio α_B/α_A controls the relative time spends each jump in layer B compared with layer A . The micro-parameter β_F determines the tendency of packets’ favour to small-degree or large-degree nodes in layer F , and reflects the micro-level difference between nodes in the same layer. Large degree (small degree) nodes in layer F are preferentially to be the next stop when $\beta_F < 0$ ($\beta_F > 0$). When $\beta_F = 0$, nodes with different degrees have the same probability to be the next stop. Fig. 1 illustrates the routing on multilayer networks.

III. THEORETICAL ANALYSIS

From the perspective of statistical physics, we use the order parameter $H(R)$ to characterize the congestion on multilayer networks [21],

$$H(R) = \lim_{t \rightarrow \infty} \frac{C}{R} \frac{\langle \Delta W \rangle}{\Delta t}, \quad (3)$$

where $\Delta W = W(t + \Delta t) - W(t)$, $\langle \dots \rangle$ is average value over Δt , and $W(t)$ is the total number of accumulated packets in the system at time t . From the varying of H with R , we will know the critical point R_c (to be computed later) above which the congestion occurs. For a small value of R , the number of generated and delivered packets are balanced, i.e., every packet can be transported to their destinations, thus $H(R) = 0$. For a large value of R (i.e., $R > R_c$), the congestion occurs and the number of accumulated packets increases with time, so $H(R) > 0$. The critical traffic capacity R_c is the most significant parameter of a transportation network, which can be used to evaluate the performance of a routing strategy, i.e., the larger, the better.

To compute the value of R_c , we first define the efficient betweenness centralities (EBC) of nodes in multilayer networks as

$$g(\alpha_F, \beta_F, v) = \sum_{s \neq t} \frac{\sigma^{st}(\alpha_F, \beta_F, v)}{\sigma^{st}(\alpha_F, \beta_F)}, \quad (4)$$

where $\sigma^{st}(\alpha_F, \beta_F)$ is the number of efficient paths between nodes s and t for given values of α_F and β_F , and $\sigma^{st}(\alpha_F, \beta_F, v)$ is the number of efficient paths that pass node v . The larger value of $g(\alpha_F, \beta_F, v)$, the more efficient paths that pass node v . As a result, node v needs to process more packets and has a larger probability to be congested. We denote nodes with high values of EBC as high-load (HL) nodes, and similarly denote nodes with low values of EBC as low-load (LL) nodes. A coupled node v^o can deliver the packets to its neighbors in both layers A and B , and it has two values of EBCs $g(\alpha_F, \beta_F, v_A^o)$ and $g(\alpha_F, \beta_F, v_B^o)$, where v_A^o (v_B^o) represents node v^o in layer A (B). If node v_A^o or v_B^o overload, traffic congestion will occur at node v^o . Thus, node v^o 's EBC in the system is the maximum value of $g(\alpha_F, \beta_F, v_A^o)$ and $g(\alpha_F, \beta_F, v_B^o)$, i.e., $g(\alpha_F, \beta_F, v^o) = \max\{g(\alpha_F, \beta_F, v_A^o), g(\alpha_F, \beta_F, v_B^o)\}$. For a non-coupled node v_A (i.e., node v_A has no counterpart in layer B), it can only deliver the packets to neighbors in layer A , and its EBC can be expressed as $g(\alpha_F, \beta_F, v_A)$.

At every time step, the system will generate R packets in layer A . We can get the average number of packets that a node v needs to process as

$$\langle \Theta_F \rangle = R \frac{g(\alpha_F, \beta_F, v)}{N_A(N_A - 1)}. \quad (5)$$

When $R \leq R_c$, there is no accumulated packets at any node in the system, i.e., $\langle \Theta_F \rangle \leq C$. When $R > R_c$, traffic congestion will occur at some HL nodes, i.e., $\langle \Theta_F \rangle > C$. Since the node with the largest EBC value has the largest probability being congested, and combining the condition $C = 1$, the critical packet generating number R_c should fulfill

$$R_c = \frac{N_A(N_A - 1)}{g_{\max}(\alpha_F, \beta_F)}, \quad (6)$$

where $g_{\max}(\alpha_F, \beta_F)$ is the largest value of EBC in the system for the given α_F and β_F .

IV. RESULTS

We introduce four parameters to investigate the effectiveness of CMR strategy. First, we introduce a generalized parameter coupling based on Ref. [40], which is used to describe how well two layers are used to transmit the packets. Here the coupling is defined as

$$\lambda = \frac{\sum_{s \neq t} \sigma_B^{st}(\alpha_F, \beta_F)}{\sum_{s \neq t} \sigma^{st}(\alpha_F, \beta_F)}, \quad (7)$$

where $\sigma^{st}(\alpha_F, \beta_F)$ is the number of efficient paths between nodes s and t for given values of α_F and β_F , and $\sigma_B^{st}(\alpha_F, \beta_F)$ is the number of efficient paths that contains at least one edge in layer B . Specifically, we have $\sigma_B^{st}(\alpha_F, \beta_F) = 0$ when every efficient path between nodes s and t only uses the edges in layer A . For the case of $\lambda \approx 0$, most packets are transported only by layer A , without using the edges in layer B . With the increase of λ , more packets are transported by using the edges in B .

Secondly, we define δ as

$$\delta = \frac{\sum_{s \neq t} e_B^{st}(\alpha_F, \beta_F)}{\sum_{s \neq t} e_A^{st}(\alpha_F, \beta_F)}, \quad (8)$$

where $e_A^{st}(\alpha_F, \beta_F)$ [$e_B^{st}(\alpha_F, \beta_F)$] is the number of edges belonging to layer A (B) in the efficient paths between nodes s and t for given values of α_F and β_F . When $\delta \approx 0$, most edges that are used to deliver packets belong to layer A . The more edges in layer B are used to transport packets, the larger value of δ . The definitions of λ and δ look similar, the difference is that coupling λ represent the proportion of all the efficient paths in system that contain edges in layer B , while δ is that, in all efficient paths, the ratio of edges in B and A .

Thirdly, we define the average length of efficient paths to capture the effectiveness of the CMR strategy as

$$\langle d \rangle = \frac{1}{N_A(N_A - 1)} \sum_{s \neq t} d^{st}(\alpha_F, \beta_F), \quad (9)$$

where $d^{st}(\alpha_F, \beta_F)$ is the length or jumps of efficient paths between node s and t for given values of α_F and β_F . For example, the length of selected path between nodes s and t in Fig. 1 is 3. The smaller of $\langle d \rangle$, the less average jumps of the packets arrive the destination.

To improve network traffic capacity, the average packet delivery time $\langle T \rangle$ must be minimized. The definition of $\langle T \rangle$ is

$$\langle T \rangle = \lim_{t \rightarrow \infty} \frac{1}{n} \sum_{p=1}^n T_p, \quad (10)$$

where n is the number of arrived packets at a given time and T_p is the packet delivery time of packet p . The delivery time of each packet consists of the travelling time from the origin to the destination and the waiting time in the queue of the congested nodes. When R is less than R_c , $\langle T \rangle$ only depends on the travelling time which is relatively small, while when $R > R_c$, $\langle T \rangle$ increases with R rapidly.

A. Artificial multilayer networks

In this subsection, we perform extensive numerical simulations on artificial multilayer networks. We set the size of layer A as $N_A = 1000$, degree exponents $\gamma = 3.0$, the minimum degree $k_{\min} = 2$, and the maximum degree $k_{\max} \sim \sqrt{N_A}$. The size of layer B is $N_B = 500$ and average degree $\langle k_B \rangle = 6$. All the results are obtained by averaging over 20 different network realizations, with 100 independent runs on each realization.

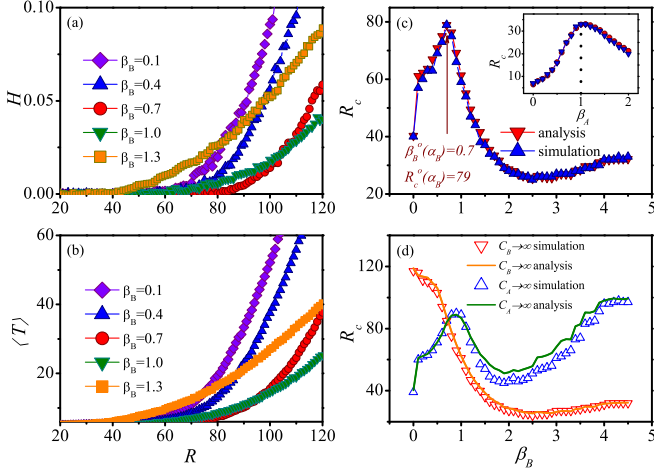


FIG. 2: The efficiency of CMR strategy on artificial multilayer networks when $\alpha_B = 0.5$. (a) The order parameter H and (b) the average delivery time $\langle T \rangle$ of packets versus R . (c) The traffic capacity R_c of multilayer networks and (d) the upper limit capacity of layer B (A) as a function of the β_B . The inset of (c) is the traffic capacity R_c of monolayer networks (layer A) as a function of β_A when $\alpha_A = 1$. The theoretical analysis results are obtained from Eq. (6). We set other parameters as $N_A = 1000$, $\gamma = 3.0$, $k_{\min} = 2$, $k_{\max} \sim \sqrt{N_A}$, $N_B = 500$, $\langle k_B \rangle = 6$, $\alpha_A = 1$, and $\beta_A = 1$.

We first focus on the effects of micro-parameter β_B on the effectiveness of CMR strategy in Fig. 2. Since $\beta_A = 1$ is optimal value without layer B for the case of $\alpha_A = 1$ [see the inset of Fig. 2(c)], we set $\alpha_A = 1$ and $\beta_A = 1$. Through extensive numerical simulations, we find that other values of α_A and β_A do not qualitatively affect the effectiveness of the proposed CMR strategy. We set $\alpha_B/\alpha_A < 1$ (i.e., $\alpha_B \leq 1$) here, which indicates that a journey on the high speed layer B is favored for a journey in layer A . From Figs. 2(a) and (b), we find that for different values of micro-parameter β_B , both the order parameter H and average packet delivery time $\langle T \rangle$ monotonically increases with R . Above the threshold R_c , H and $\langle T \rangle$ are finite, and increase with R . Importantly, we find that R_c exhibits a non-monotonously varying with β_B as shown in Fig. 2(c), and the system exists an optimal value $\beta_B^o(\alpha_B) = 0.7$ at which the traffic capacity R_c reaches the maximum value $R_c^o(\alpha_B) = 79$ when $\alpha_B = 0.5$. The average length of efficient paths $\langle d \rangle$ reaches the minimum value at the same parameters [see Fig. 3(c)]. Specifically, R_c first increases with β_B , and peaks at $\beta_B^o(\alpha_B) = 0.7$, and then decreases. The theoretical predictions agree well with the numerical values

of R_c . To understand the non-monotonous phenomenon, we need to check what happens when varying β_B . When β_B is small (large), the values of λ and δ are large (small) as shown in Figs. 3(a) and (b). This indicates that packets are more likely to be transmitted in layer B (A). For a small value of β_B , many coupled nodes are used to transmit packets. Similar to the effective strategy on monolayer networks, preferentially transmitting the packets through small degree nodes in layer B could improve the traffic capacity of the system [21], and R_c thus first increases with β_B . For a large value of β_B , most packets are transmitted on layer A , which decreases the usage of coupled nodes in transmitting the packets, and R_c thus decreases. In Fig. 2(d), we further verify in which layer the congestion occurs for different values of β_B . To this end, we set the delivery ability of nodes in layer A (B) is infinite when we check the upper limit capacity of layer B (A), i.e., $C_A \rightarrow \infty$ and $g(\alpha_F, \beta_F, v^o) = g(\alpha_F, \beta_F, v_B^o)$ [$C_B \rightarrow \infty$ and $g(\alpha_F, \beta_F, v^o) = g(\alpha_F, \beta_F, v_A^o)$]. We find that congestion occurs in layer B (A) for small (large) values of β_B , since layer B (A) has a smaller critical network throughput. From what we discussed above, we can see that compared to the isolated low speed network A , the capacity R_c of multilayer network is remarkably improved at some parameters, since the traffic load of the low speed layer A is redistributed to the high speed layer B reasonably. The system capacity is affected by both layers A and B , and depends non-monotonically on micro-parameter β_B . The theoretical predictions agree well with the numerical simulations in both Figs. 2(c) and (d).

We further study the effects of network size N_B and average degree $\langle k_B \rangle$ of layer B (i.e., increasing the number of coupled nodes and edges in the high speed network) on system capacity in Fig. 4. As shown in Figs. 4(a) and (c), we find that the maximum traffic capacity $R_c^o(\alpha_B)$ when $\alpha_B = 0.5$ increases with $\langle k_B \rangle$ and N_B , since the number of efficient paths (coupled nodes) increase. That's to say, increasing the size and average degree of the high speed layer enhance the traffic capacity of multilayer networks effectively. We note that the optimal micro-parameter $\beta_B^o(\alpha_B)$ decreases with $\langle k_B \rangle$ [see Fig. 4(b)], but does not change with N_B [see Fig. 4(d)]. Again, our theoretical predictions agree well with the numerical simulations.

All results above are obtained when macro-parameter $\alpha_B = 0.5$, we next study the effects of macro-parameter α_B in Fig. 5. We find that $R_c^o(\alpha_B)$ depends non-monotonically on α_B [$R_c^o(\alpha_B)$ first increase with α_B and then decrease], and the corresponding optimal micro-parameter $\beta_B^o(\alpha_B)$ monotonically decreases with α_B and reaches a suitable packets' preference to layer B . For small (large) values of α_B , λ and δ are large (small) as shown in the insets of Figs. 5(a) and (b) respectively. Importantly, we find that the system reaches a maximum traffic capacity R_c^* at the optimal macro- and micro-level parameters combination (α_B^*, β_B^*) , and the number of delivered packets by each layer reach to a balance. From Figs. 5(a) and (b), we obtain $R_c^* = 79$ at $(\alpha_B^*, \beta_B^*) = (0.5, 0.7)$. Without the high speed network B , the maximum traffic capacity of low speed network is 33 [see the inset of Fig. 2(b)]. The maximum traffic capacity of system is improved about 2.5 times once the network B is in-

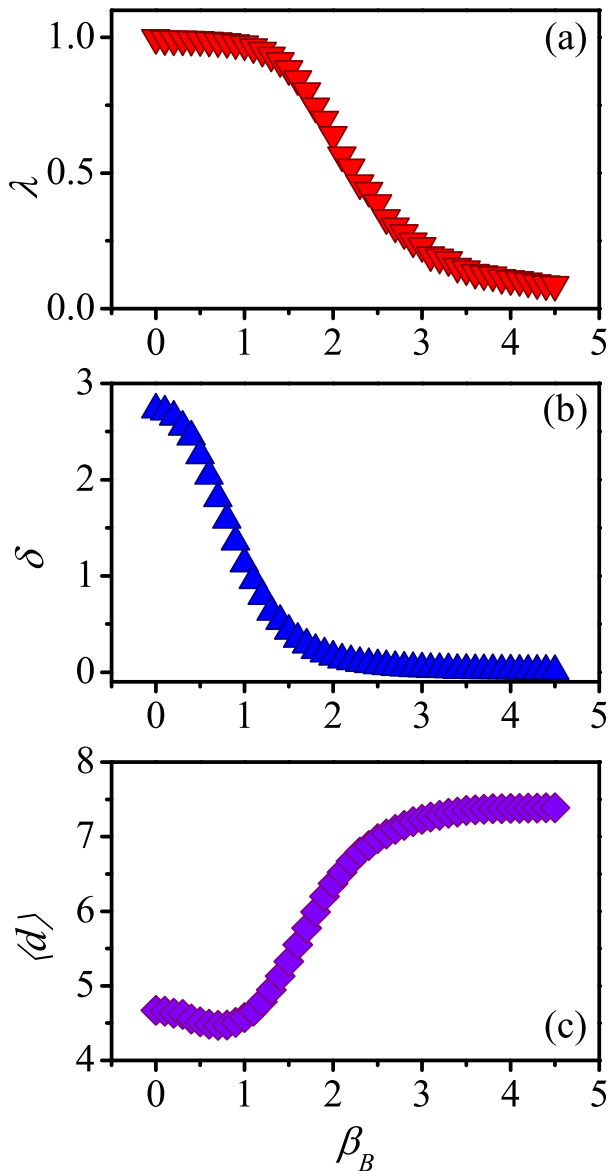


FIG. 3: The parameters (a) coupling λ , (b) ratio of edges that used in layers B and A δ , and (c) average jumps $\langle d \rangle$ between nodes VS β_B on artificial multilayer networks. We set other parameters as $N_A = 1000$, $\gamma = 3.0$, $k_{\min} = 2$, $k_{\max} \sim \sqrt{N_A}$, $N_B = 500$, $\langle k_B \rangle = 6$, $\alpha_A = 1$, $\beta_A = 1$, and $\alpha_B = 0.5$.

duced. Although establishing high speed transportation can improve the traffic capacity of low speed network, our results indicate that a reasonable redistribution of traffic load is an essential issue. The theoretical predictions agree well with the numerical simulations.

B. Real-world networks

A wide range of systems in the real world have multiple subsystems and layers of connectivity, which can be described as multilayer networks [32–35]. We verify the ef-

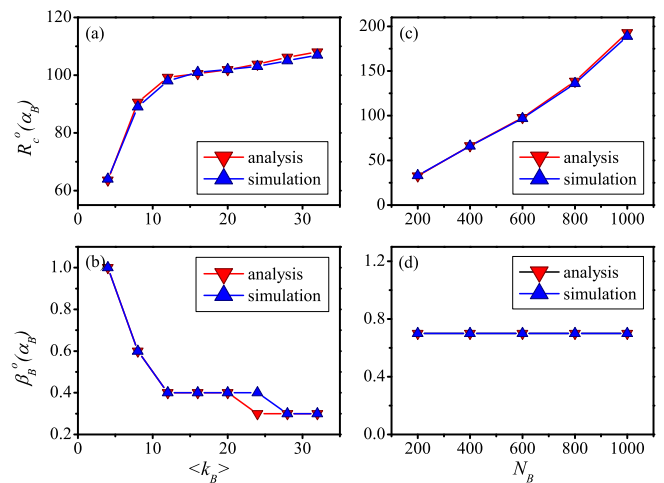


FIG. 4: CMR strategy on artificial multilayer networks with different $\langle k_B \rangle$ and N_B . The maximum capacity $R_c^o(\alpha_B)$ (top), and the corresponding optimal micro-parameter $\beta_B^o(\alpha_B)$ (bottom) as a function of $\langle k_B \rangle$ [(a) and (b)] and N_B [(c) and (d)]. We set other parameters as $N_A = 1000$, $\gamma = 3.0$, $k_{\min} = 2$, $k_{\max} \sim \sqrt{N_A}$, $\alpha_A = 1$, $\beta_A = 1$, $\alpha_B = 0.5$, $N_B = 500$ [(a) and (b)], $\langle k_B \rangle = 6$ [(c) and (d)].

TABLE I: Structural properties of Work network and Facebook network, including number of nodes N , number of edges E , mean degree $\langle k \rangle$, maximum degree k_{\max} , degree heterogeneity $H_k = \langle k^2 \rangle / \langle k \rangle^2$, diameter D , average shortest distance L , correlation coefficient r , clustering coefficient c , and modularity Q .

Network	N	E	$\langle k \rangle$	k_{\max}	H_k	D	L	r	c	Q
Work	60	194	6.5	27	1.7	4	2.4	-0.218	0.64	0.46
Facebook	32	124	7.8	15	2.3	4	2.0	0.003	0.54	0.34

fectiveness of our proposed CMR strategy on a real-world multilayer network, which is a social network of Employees of Computer Science Department (ECSD) at Aarhus University [50]. The multilayer social network consists of five kinds of online and offline relationships (Facebook, Leisure, Work, Co-authorship, Lunch), and we choose the Work and Facebook relationships as layer A and layer B , respectively. We denote this real-world network as Work-Facebook multilayer network. Layer A composes of 60 nodes and 194 edges, and layer B has 32 nodes and 124 edges. Some structural properties of the two networks are presented in Table I.

We study the effectiveness of the CMR strategy on the Work-Facebook multilayer network in Fig. 6. Since the extremely complicated structures of networks, there has two peaks of R_c versus β_B , at which the traffic capacity is very large, and the $R_c^o(\alpha_B)$ corresponds to the second peak. Compared to the isolated Work network, the capacity R_c of Work-Facebook multilayer network are improved when Facebook network joins in the system [see the inset of Fig. 6(a)], and the system capacity is affected by both Work and Facebook networks [see Fig. 6(b)]. In Fig. 7, we find that $R_c^o(\alpha_B)$ versus α_B exhibits a nonmonotonic pattern [see Fig. 7(a)], and the corresponding optimal micro-parameter $\beta_B^o(\alpha_B)$ monotonically decreases with α_B [see Fig. 7(b)]. Similar to the ar-

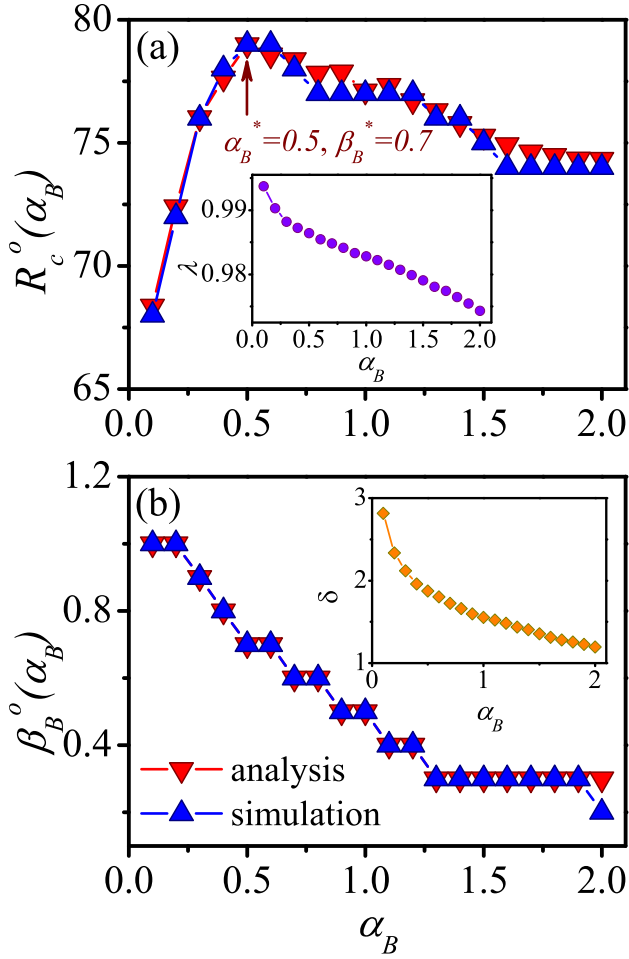


FIG. 5: CMR strategy on artificial multilayer networks with different α_B . (a) $R_c^o(\alpha_B)$ and (b) $\beta_B^o(\alpha_B)$ as a function of α_B . The insets of (a) and (b) respectively exhibit λ and δ versus α_B when $\beta_B = \beta_B^o(\alpha_B)$. We set other parameters as $N_A = 1000$, $\gamma = 3.0$, $k_{\min} = 2$, $k_{\max} \sim \sqrt{N_A}$, $N_B = 500$, $\langle k_B \rangle = 6$, $\alpha_A = 1$, $\beta_A = 1$.

tificial networks, we find that the system reaches a maximum traffic capacity $R_c^* = 15$ at the optimal micro- and macro-level parameters $(\alpha_B^*, \beta_B^*) = (2.1, 0.7)$. The fluctuation of curves in Figs. 6 and 7 is caused by the extremely complicated structures of both Work and Facebook networks. We should note that the theoretical predictions markedly well agree with the numerical simulations.

V. DISCUSSIONS

For the purpose of alleviating the congestion of a low speed transportation network, an intuitive way is to build a new high speed network in busy regions or among the high flow nodes. The low and high speed networks constitute a multilayer network. How to reasonable redistribution of traffic load to maximize the multilayer network is an essential issue and full of challenges. In this work, we first proposed a comprehensive multilayer network routing (CMR) strategy

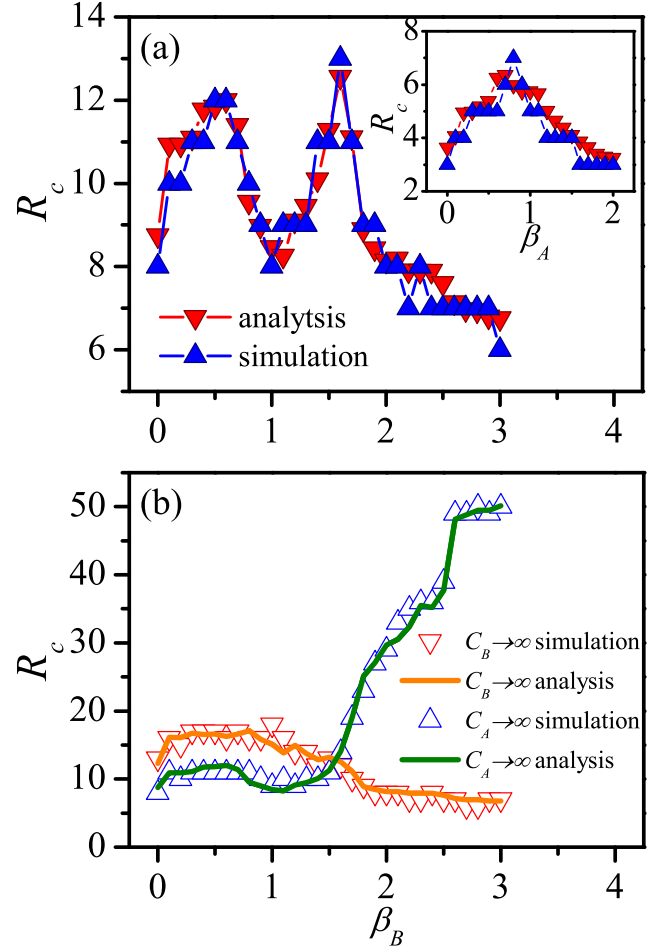


FIG. 6: CMR strategy on Work-Facebook multilayer network with $\alpha_B = 0.5$. (a) The traffic capacity R_c , and (b) the upper limit capacity of layer A (Work) and layer B (Facebook) as a function of the β_B . The inset of (a) is the traffic capacity R_c of isolated Work network as a function of β_A when $\alpha_A = 1$. We set $\alpha_A = 1$, $\beta_A = 1$, and $\alpha_B = 0.5$.

by considering different transmission speeds of layers from the macroscopic view (by adjusting a macro-parameter α_F), and different roles of nodes from the perspective of microscopic structure (controlled by a adjustable micro-parameter β_F). We then performed extensive numerical simulations on both artificial and real-world networks. We found that our routing strategy can redistribute the traffic load in low speed layer to high speed layer reasonably, and the traffic capacity of multilayer network are remarkably enhanced compared with the monolayer low speed network. In addition, the system capacity is affected by both layers A and B, and depends non-monotonically on micro-parameter β_B and macro-parameter α_B . For a given multilayer network, the system reaches a maximum traffic capacity R_c^* at the optimal micro- and macro-level parameters (α_B^*, β_B^*) . Moreover, we found that increasing the size and the average degree of the high speed layer B enhances the transport capacity of multilayer

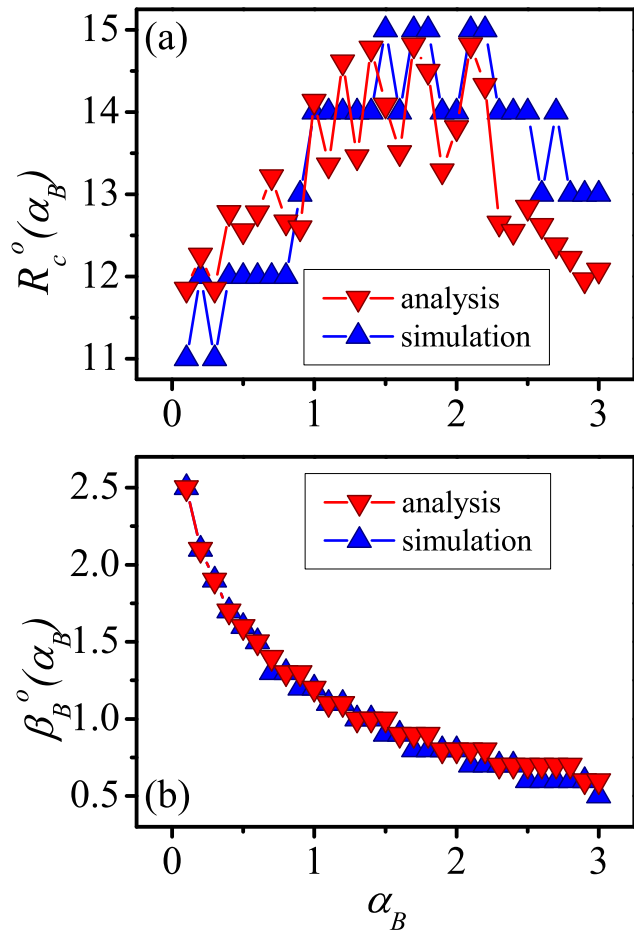


FIG. 7: CMR strategy on Work-Facebook multilayer network with different α_B . (a) The maximum capacity $R_c^o(\alpha_B)$ for a given α_B , and (b) the corresponding optimal micro-parameter $\beta_B^o(\alpha_B)$ as a function of macro-parameter α_B . We set $\alpha_A = 1$, $\beta_A = 1$.

networks more effectively. The theoretical predictions agree well with the numerical simulations in both artificial and real-world networks.

A wise way to alleviate traffic congestion for multilayer networks is designing effective multilayer network routing strategy. Our results exhibit a way to reasonable redistribute the traffic load. In this work, we proposed an effective strategy which considers the local structures of different nodes, as well as the transmission speeds of different layers. We study our proposed strategy on multilayer networks including two layers, and it can remarkably improve the systems' traffic capacity. Our research may stimulate future studies on designing realistic transportation and communication multilayer networks, such as, considering different delivery abilities of nodes, limited traffic resources, transmission cost of layers, and multilayer networks with more than two layers.

Acknowledgments

This work was supported by the National Natural Science Foundation of China (Grant Nos. 11575041 and 61673086), and the Fundamental Research Funds for the Central Universities (Grant No. ZYGX2015J153).

-
- [1] S. H. Strogatz, *Nature* **410**, 268 (2001).
 - [2] R. Albert and A.-L. Barabási, *Reviews of modern physics* **74**, 47 (2002).
 - [3] S. Boccaletti, V. Latora, Y. Moreno, M. Chavez, and D.-U. Hwang, *Physics reports* **424**, 175 (2006).
 - [4] M. Newman, *Networks: an introduction* (Oxford university press, 2010).
 - [5] A.-L. Barabási, *Network science* (Cambridge University Press, 2016).
 - [6] A. Arenas, A. Díaz-Guilera, and R. Guimera, *Physical Review Letters* **86**, 3196 (2001).
 - [7] L. Zhao, Y.-C. Lai, K. Park, and N. Ye, *Physical Review E* **71**, 026125 (2005).
 - [8] Z. Wu, L. A. Braunstein, S. Havlin, and H. E. Stanley, *Physical review letters* **96**, 148702 (2006).
 - [9] D. De Martino, L. Dall'Asta, G. Bianconi, and M. Marsili, *Physical Review E* **79**, 015101 (2009).
 - [10] M. Barthélemy, *Physics Reports* **499**, 1 (2011).
 - [11] J. Wu, K. T. Chi, F. C. Lau, and I. W. Ho, *IEEE Transactions on Circuits and Systems I: Regular Papers* **60**, 3303 (2013).
 - [12] R. Guimera, A. Arenas, A. Díaz-Guilera, and F. Giralt, *Physical Review E* **66**, 026704 (2002).
 - [13] R. Guimera, A. Díaz-Guilera, F. Vega-Redondo, A. Cabrales, and A. Arenas, *Physical Review Letters* **89**, 248701 (2002).
 - [14] B. Danila, Y. Yu, J. A. Marsh, and K. E. Bassler, *Physical Review E* **74**, 046106 (2006).
 - [15] B. Danila, Y. Yu, J. A. Marsh, and K. E. Bassler, *Chaos: An Interdisciplinary Journal of Nonlinear Science* **17**, 026102 (2007).
 - [16] Z. Liu, M.-B. Hu, R. Jiang, W.-X. Wang, and Q.-S. Wu, *Physical Review E* **76**, 037101 (2007).
 - [17] G.-Q. Zhang, D. Wang, and G.-J. Li, *Physical Review E* **76**, 017101 (2007).
 - [18] Y. Xia and D. Hill, *EPL (Europhysics Letters)* **89**, 58004 (2010).
 - [19] L. Xiang, H. Mao-Bin, L. Jian-Cheng, D. Jian-Xun, and S. Qin, *Chinese Physics B* **22**, 018904 (2013).
 - [20] G.-Q. Zhang, S. Zhou, D. Wang, G. Yan, and G.-Q. Zhang, *Physica A: Statistical Mechanics and its Applications* **390**, 387 (2011).
 - [21] G. Yan, T. Zhou, B. Hu, Z.-Q. Fu, and B.-H. Wang, *Physical*

- Review E **73**, 046108 (2006).
- [22] M. Tang, Z. Liu, X. Liang, and P. Hui, *Physical Review E* **80**, 026114 (2009).
- [23] B. Tadić and M. Mitrović, *The European Physical Journal B* **71**, 631 (2009).
- [24] X. Ling, M.-B. Hu, R. Jiang, and Q.-S. Wu, *Physical Review E* **81**, 016113 (2010).
- [25] M. Tang and T. Zhou, *Physical review E* **84**, 026116 (2011).
- [26] A. Rachadi, M. Jedra, and N. Zahid, *Chaos: An Interdisciplinary Journal of Nonlinear Science* **23**, 013114 (2013).
- [27] Y. Gan, M. Tang, and H. Yang, *The European Physical Journal B* **86**, 1 (2013).
- [28] P. Echenique, J. Gómez-Gardeñes, and Y. Moreno, *Physical Review E* **70**, 056105 (2004).
- [29] P. Echenique, J. Gómez-Gardenes, and Y. Moreno, *EPL (Europhysics Letters)* **71**, 325 (2005).
- [30] Z.-X. Wu, W.-X. Wang, and K.-H. Yeung, *New Journal of Physics* **10**, 023025 (2008).
- [31] W.-X. Wang, Z.-X. Wu, R. Jiang, G. Chen, and Y.-C. Lai, *Chaos: An Interdisciplinary Journal of Nonlinear Science* **19**, 033106 (2009).
- [32] J. Gao, S. V. Buldyrev, H. E. Stanley, and S. Havlin, *Nature physics* **8**, 40 (2012).
- [33] M. Kivelä, A. Arenas, M. Barthelemy, J. P. Gleeson, Y. Moreno, and M. A. Porter, *Journal of complex networks* **2**, 203 (2014).
- [34] K.-M. Lee, B. Min, and K.-I. Goh, *The European Physical Journal B* **88**, 1 (2015).
- [35] S. Boccaletti, G. Bianconi, R. Criado, C. I. Del Genio, J. Gómez-Gardeñes, M. Romance, I. Sendiña-Nadal, Z. Wang, and M. Zanin, *Physics Reports* **544**, 1 (2014).
- [36] S. V. Buldyrev, R. Parshani, G. Paul, H. E. Stanley, and S. Havlin, *Nature* **464**, 1025 (2010).
- [37] W. Wang, M. Tang, H. Yang, Y. Do, Y.-C. Lai, and G. Lee, *Scientific reports* **4**, 5097 (2014).
- [38] J. Gómez-Gardenes, I. Reinares, A. Arenas, and L. M. Floría, *Scientific reports* **2**, 620 (2012).
- [39] J. Aguirre, R. Sevilla-Escoboza, R. Gutiérrez, D. Papo, and J. Buldú, *Physical review letters* **112**, 248701 (2014).
- [40] R. G. Morris and M. Barthelemy, *Physical review letters* **109**, 128703 (2012).
- [41] J. Zhou, G. Yan, and C.-H. Lai, *EPL (Europhysics Letters)* **102**, 28002 (2013).
- [42] O. Yagan, D. Qian, J. Zhang, and D. Cochran, *IEEE Journal on Selected Areas in Communications* **31**, 1038 (2013).
- [43] F. Tan, J. Wu, Y. Xia, and K. T. Chi, *Physical Review E* **89**, 062813 (2014).
- [44] A. Solé-Ribalta, S. Gómez, and A. Arenas, *Physical review letters* **116**, 108701 (2016).
- [45] M. Li, M.-B. Hu, and B.-H. Wang, *arXiv preprint arXiv:1607.05382* (2016).
- [46] C. D. Brummitt, R. M. DSouza, and E. Leicht, *Proceedings of the National Academy of Sciences* **109**, E680 (2012).
- [47] C.-G. Gu, S.-R. Zou, X.-L. Xu, Y.-Q. Qu, Y.-M. Jiang, H.-K. Liu, T. Zhou, et al., *Physical Review E* **84**, 026101 (2011).
- [48] M. Catanzaro, M. Boguñá, and R. Pastor-Satorras, *Physical Review E* **71**, 027103 (2005).
- [49] P. Erdős and A. Rényi, *Publ. Math. Inst. Hungar. Acad. Sci* **5**, 17 (1960).
- [50] M. Magnani, B. Micenkova, and L. Rossi, *arXiv preprint arXiv:1303.4986* (2013).